# An Indirect AC-AC Converter With Power Factor Correction and High Frequency Insulation

Emerson J. A. da Silva
*Electrical Engineering Department*
*Federal University of Ceará (UFC)*
Fortaleza, Brazil
emmersonjimmy@hotmail.com

Bruno R. de Ameida
*Electrical Engineering Department*
*University of Fortaleza (Unifor)*
Fortaleza,Brazil
almeida@unifor.br

Paulo P. Praça
*Electrical Engineering Department*
*Federal University of Ceará (UFC)*
Fortaleza, Brazil
paulopp@dee.ufc.br

Demercil de S. Oliveira Jr.
*Electrical Engineering Department*
*Federal University of Ceará (UFC)*
Fortaleza,Brazil
demercil@dee.ufc.br

Luiz H. S. C. Barreto
*Electrical Engineering Department*
*Federal University of Ceará (UFC)*
Fortaleza,Brazil
paulopp@dee.ufc.br

Fernando Luiz Marcelo Antunes
*Electrical Engineering Department*
*Federal University of Ceará (UFC)*
Fortaleza,Brazil
fantunes@dee.ufc.b

***Abstract*— This paper proposes an indirect AC-AC converter with Power Factor Correction (PFC) and high frequency isolation. The proposed topology is based on the Dual Active Bridge (DAB) converter in the three state switching cell. The proposed converter has a high power factor, low Total Harmonic Distortion (THD), fast dynamic response and power flow control between the rectifier and the inverter stage. The power flow control is performed through the phase-shit technique. The design of the controllers used by the converter and experimental results are presented.**

***Keywords—AC-AC Converter, PFC, Dual Active Bridge, Phase-shift***

## I. INTRODUCTION

Initially, the AC-AC power conversion was based on semiconductors with low switching frequency. In industry, the tradicional way is to use AC thyristor power controllers, which can produce the desired output voltage by implementing the phase angle or integral cycle control on input AC voltage. However, the AC thyristor controller have several disadvantages such as low power factor, large total harmonic distortion in source current and lower efficiency [1]. In the last decades, the use Metal Oxide Semiconductor Field Effect Transistor (MOSFET), Insulated Gate Bipolar Transistor (IGBT) and Pulse Width Modulation (PWM) has been employed in AC-AC converters, allowing news topologies. The AC Choppers, Matrix converters and AC-DC-AC converters with DC-links are employed, because of their better power factor and efficiency with relatively smaller filter requirements [2]. Therefore, it is necessary to have a classification of the AC-AC converters. In [3] it presents a classification of the converters according to the transfer of energy between the input and output terminals, in direct and indirect. Direct converters have a single stage of energy processing or has no intermediate energy storage elements and indirect converters have double conversion or has intermediate energy storage elements.

The AC Choppers are direct converters derived from traditional DC-DC converters, such as the buck, boost, buck-boost and so forth [4]. These converters allow only the control of the amplitude of the output voltage without changing the frequency, different from the cycloconverters and matrix converters [5]. Due to the use of the PWM technique and the use of high frequency switches, AC choppers have become an attractive solution for Flexible Alternating Current Transmission (FACTS) and voltage control of sensitive loads due to the ability to reject input voltage disturbances [6].

Denoted by [7], the Conventional Matrix Converters (CMC) have direct energy conversion, because each input phase can be directly connected to the output phase without intermediate elements of energy storage. The Matrix converter has been considered a future concept converter for speed control of motors and applications in renewable energy [8]. However, Matrix converters require bi-directional switches in current and voltage, totaling 18 semiconductor switches. The maximum voltage available at the output is 86.6% of the input voltage [9].

The Indirect Matrix Converters (IMC) consists of two conversion stages. However, the indirect converter does not have an intermediate energy storage element, the link between the rectifier stage and the inverter stage is direct [10]. The Matrix converters have as advantages high energy processing density and have no dc link capacitors [11].

Back-to-back converters with dc link are used in the industry due to their step-up and step-down characteristic of output voltage [12]. A rectifier source voltage in the input and inverter voltage source in the output forms the back-to-back converters. The dc link provides a decoupling between the input and output stage, and allows internal energy storage for applications that have fast dynamic response. However, the dc link capacitors are bulk and responsible for reducing the life of the converter.

The Dual Active Bridge (DAB) converters are widely used in modern energy conversion systems that require bi-directional energy transfer [13]. On the other hand, the topology of the DAB AC-AC converter is also interesting for the application with high power quality and high power density.

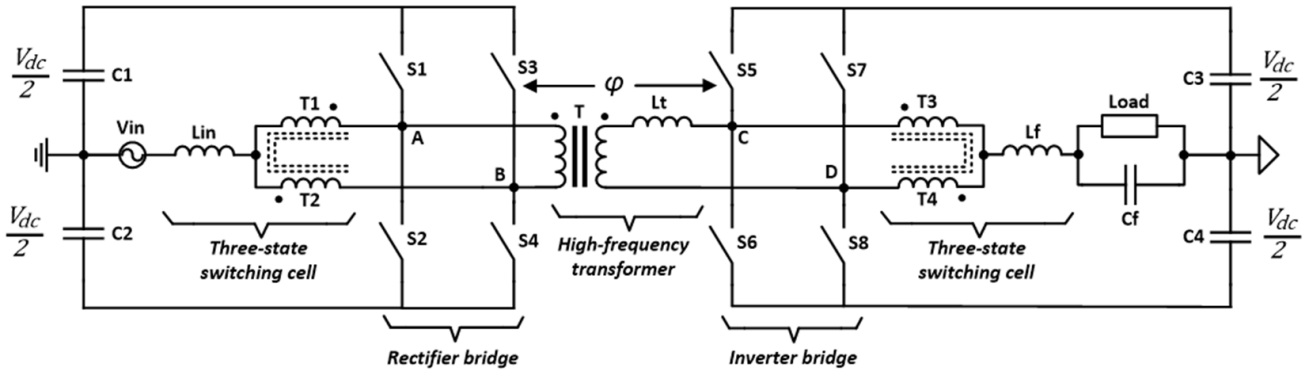


Fig. 1. Proposed topology.

## II. Proposed Topology

The proposed topology is presented in Fig. 1. The converter is based on the DAB converter [14] and the three-state switching cell (3SSC) [15]. The use of 3SSC aims to reduce switching and conduction losses, reduction of input and output filters, because the frequency in the magnetic elements is twice the frequency of switching [16].

The topology consists of two symmetric converters, an AC-DC converter and an DC-AC converter. As the energy conversion process features double conversion and energy storage elements, the converter is indirect

The AC-DC converter is a rectifier with Power Factor Correction (PFC), that is, has sinusoidal input current with low harmonic distortion, resulting in high power factor. The output voltage of the inverter is sinusoidal with fixed frequency and low harmonic distortion. In addition, the voltage is set according to reference and provides fast dynamic response to linear and non-linear load changes.

The power flow between the power grid and the load is performed by the phase shift technique [17]. The primary side voltage of the high frequency transformer is displaced from the secondary side voltage by φ, allowing the power flow from the rectifier to the inverter.

## III. Modulation Technique

The modulation technique used in the rectifier and inverter is Sinusoidal Pulse Width Modulation (SPWM). The Table I shows the possible states of the switches of the proposed converter.

TABLE I. Analysis of The Switching States For The Converter.

| Switching States for the Converter | | | | | | |
|---|---|---|---|---|---|---|
| **Vi/Vo** | ***Switching States*** | | | | ***Voltage*** | |
| | **S1/S5** | **S2/S6** | **S3/S7** | **S4/S8** | **Vab/Vcd** | **Va'/Vb'** |
| Positive semi-cycle | 1 | 0 | 0 | 1 | +Vdc | 0 |
| | 1 | 0 | 1 | 0 | 0 | +Vdc/2 |
| | 0 | 1 | 1 | 0 | -Vdc | 0 |
| Negative semi-cycle | 1 | 0 | 0 | 1 | +Vdc | 0 |
| | 0 | 1 | 0 | 1 | 0 | -Vdc/2 |
| | 0 | 1 | 1 | 0 | -Vdc | 0 |

The control of the power flow is accomplished through the phase shift technique. Thus, by modifying the displacement angle between the carrier waves of the rectifier and the inverter, the direction of the power flow is determined. Fig. 2 shows the main waveforms associated with the modulation technique used. Analyzing the figure, it identifies that the carrier waves are fixed and displaced by 180° for each leg of the bridge. On the other hand, the carrier on the inverter side is displaced from φ. Thus, the use of this technique allows the voltages in the transformer to be a square wave of three levels, + Vdc, 0 and –Vdc.

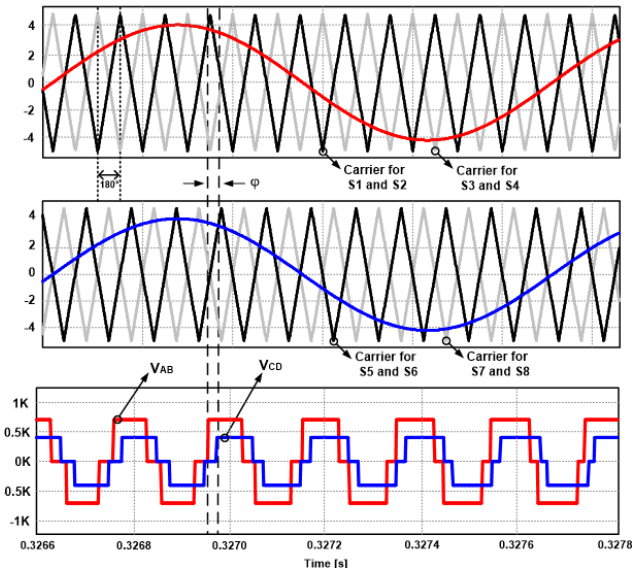


Fig. 2. Modulation technique employed.

## IV. Determination of Passive Components of Rectifier

Tab. II shows the specifications used to calculate the input inductor and dc bus capacitors.

TABLE II. Specifications For Determination of Passive Components of Rectifier

| Specifications of Rectifier | | | |
|---|---|---|---|
| DC bus Voltage | $[V_{DC,r}]$ | 700 | V |
| Switching Frequency | $[f_{sw,r}]$ | 20 | kHz |
| Output Power | $[P_{o,r}]$ | 1 | kW |
| Ripple Current on Inductor | $[\Delta I_{L,r}]$ | 1 | A |
| Ripple Voltage on Capacitors | $[\Delta V_{C,r}]$ | 20 | V |
| Hold-up time | $[\Delta t_{,r}]$ | 8,33 | ms |

### A. *Inductor - $L_R$*

Equation (1) is used to determine the input inductance of the AC-DC converter. The ripple frequency of the current is twice the switching frequency, due to the three state switching cell.

$$L_R = \frac{V_{DC,r}}{16 \cdot \Delta I_{L,r} \cdot 2 \cdot f_{sw,r}} \quad (1)$$

### B. *Capacitor - $C_{DC,r}$*

The dc bus is constituted by a central point structure, as shown in Fig. 01. The value of each capacitor is determined by expression (2).

$$C_{DC,r} = \frac{P_{o,r}\Delta_{t,r}}{\left(\frac{V_{DC,r}}{2}\right)^2 + \left(V_{DC,max} - \Delta V_{C,r}\right)^2} \quad (2)$$

## V. Determination of Passive Components of Inverter

Specifications used to calculate the passive components of the inverter are show in Table III.

TABLE III. Specifications For Determination of Passive Components of Inverter.

| Specifications of Inverter | | | |
|---|---|---|---|
| DC bus Voltage | [$V_{DC,i}$] | 400 | V |
| Output Voltage | [$V_{o,i}$] | 110 | V |
| Switching Frequency | [fsw,i] | 20 | kHz |
| Output Inverter | [Po,i] | 1 | kW |
| Ripple Current on Inductor | [$\Delta I_{Lf,i}$] | 2,57 | A |
| Ripple Voltage on Capacitors | [$\Delta V_{C,i}$] | 1,56 | V |
| Hold-up time | [$\Delta$t,r] | 8,33 | ms |

### A. *Inductor - $L_f$*

The inverter LC filter inductor is determined by expression (3).

$$L_f = \frac{2 \cdot \pi \cdot V_{o,i} \cdot \left[\left(V_{DC,i}/2\right) - V_{o,i}\right]}{2 \cdot \Delta I_{Lf,i} \cdot \pi \cdot f_{sw,i} \cdot V_{DC,i}} \quad (3)$$

### B. *Capacitor - $C_f$*

Equation (4) is used to calculate the output filter capacitor of the inverter according to specification required by Table III.

$$C_f = \frac{4 \cdot \pi^2 \cdot V_{o,i} \cdot \left[\left(V_{DC,i}/2\right) - V_{o,i}\right]}{16 \cdot L_f \cdot \Delta V_{Cf,i} \cdot V_{DC,i} \cdot \left(2 \cdot \pi \cdot f_{sw,i}\right)^2} \quad (4)$$

### C. *Capacitor – $C_{DC,i}$*

Since the proposed topology is symmetrical, the dc bus of the inverter is the same as the rectifier. Thus, using Equation (2) can determine the capacitors of the inverter, following the proper specifications.

## VI. Control Strategy of The Inverter

Fig. 3 shows the simplified block diagram of the control used by the rectifier. According to bock diagram, see four controllers, two voltage controllers and two current controllers.

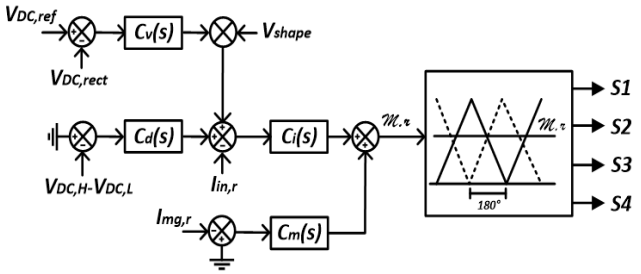


Fig. 3. Block diagram of the rectifier control.

The power factor correction is done by the control Average Current Mode Control [18], which is formed of an internal current loop and an external voltage loop. Balance the voltage in the capacitors of the dc bus is performed by the balance loop, which addition an offset to the control action of the PFC voltage controller. Additionally, it has the magnetizing current control loop on the primary side of the high frequency transformer, which will prevent the saturation of the transformer [19].

### A. *Current Controller Design (PFC)*

The k-factor method [20] is used for the controller design. The transfer function used in the current controller design of the PFC control is (5).

$$G_i(s) = \frac{I_L(s)}{d(s)} = \frac{(V_{DC}/2)}{s \cdot L_R + R_L} \quad (5)$$

For crossover frequency of 4kHz and phase margin of 45°, the PI type-II controller is designed. The zero is placed at the frequency of 1,65kHz and the polo at the frequency of 9,68kHz. Fig. 4 shows the open loop system with the PFC current controller.

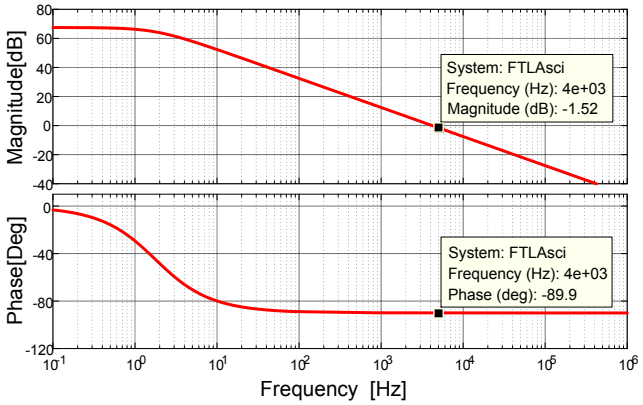


Fig. 4. Bode diagram of the closed loop system of the PFC current.

### B. *Voltage Controller Design (PFC)*

For the design of the PFC voltage controller, it uses the transfer function given by (6). The equation is formed by the dc bus voltage under the input current, resulting in the impedance Z(s).

$$Z(s) = \frac{V_{DC,r}(s)}{I_L(s)} = \frac{R_o \cdot R_{se} \cdot C_{DC,r} \cdot s + 1}{(R_o + R_{se}) \cdot C_{DC,r} \cdot s + 1} \quad (6)$$

To ensure the decoupling between the voltage and current feedback loop, assign a crossover frequency of 10Hz to the voltage loop. The desired phase margin is 60°.The zero and pole of the PI Type-II controller are located at the frequency of 3,10Hz and 32.3Hz. The bode diagram of open loop transfer function with PFC voltage controller is show in Fig. 5.

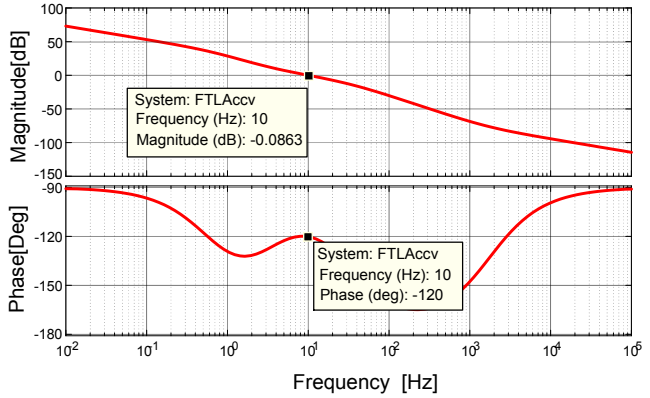


Fig. 5. Bode diagram of the closed loop system of the PFC voltage.

### C. DC bus Balance Voltage Controller Design

To ensure voltage balance in the dc bus, a voltage controller is added, as shown in the block diagram of Fig. 3. Equation (7) is the transfer function used for the controller design.

$$G_d(s) = \frac{V_c(s)}{I_d(s)} = \frac{1}{s \cdot 2 \cdot C_{DC,r}} \quad (7)$$

As the control action of the balance feedback loop is added with the control action of the feedback loop of the PFC voltage control, a crossing frequency of 5Hz is assigned. The zero and the pole frequencies are 1,32Hz and 19Hz, for phase margin of 60°. The closed loop response with the voltage controller is shown in Fig. 6.

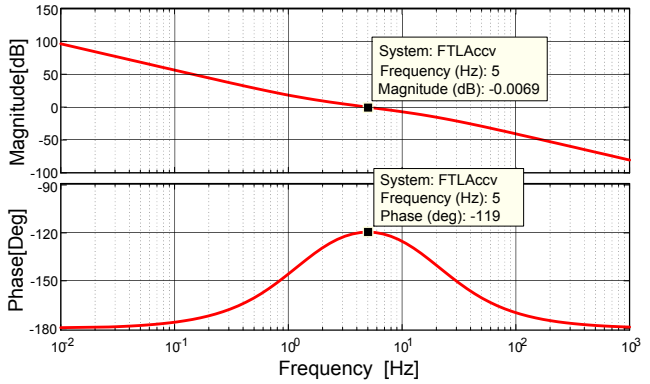


Fig. 6. Bode diagram of the closed loop system of the dc link balance voltage.

### D. Magnetizing Current Controller Design

Considering the switches are not ideal and the dead time used in the switching, it is necessary to control the magnetizing current, to avoid the saturation of the high frequency transformer. To solve this problem, auxiliary inductors are added in parallel to the transformer windings and it has ensured that the current in the inductors does not have a continuous level. Equation (8) describes the transfer function of the magnetizing current.

$$G_m(s) = \frac{I_m(s)}{d(s)} = \frac{V_{DC,r}}{s \cdot L_m} \quad (8)$$

The crossover frequency and phase margin are 240Hz and 60°. The bode diagram of the open loop transfer function with the current controller is shown in Fig. 7.

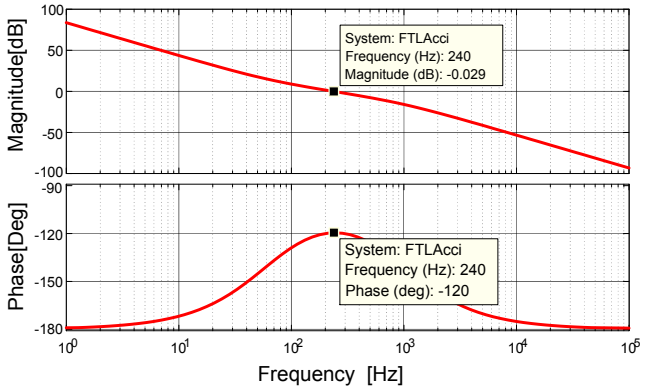


Fig. 7. Bode diagram of the closed loop system of the magnetizing current.

## VII. Control Strategy of The Inverter

The strategy employed by the inverter is composed of three control loop, as can be seen in Fig. 8. The output voltage loop ensure sinusoidal voltage, low DHT and fast dynamic response.

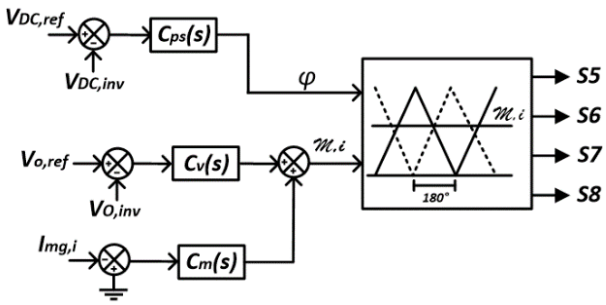


Fig. 8. Block diagram of the inverter control.

The phase-shift control loop displaced the inverter carriers by an angle φ according to the dc bus voltage. The magnetizing current control loop is necessary again to avoid secondary transformer saturation.

### A. Output Voltage Controller Design

The output voltage controller is the traditional PID. Equation (9) shows the relation between the output voltage and the duty cycle.

$$G_v(s) = \frac{V_o(s)}{d(s)} = \frac{(V_{cc}/2)}{s^2 \cdot C_f \cdot L_f + 1} \quad (9)$$

According to [21], inverters with unipolar modulation can adopt the crossing frequency equal to half the switching frequency. Thus, the crossing frequency adopted is 10kHz.The PID controller has one pole at the origin and another pole in the frequency of 143,3kHz, the double zero are

located at the frequency of 5,74kHz. The bode diagram of the open loop transfer function with the voltage controller is show in Fig. 9. It can be seen, the controller proposes zero magnitude and phase margin of approximately 30°.

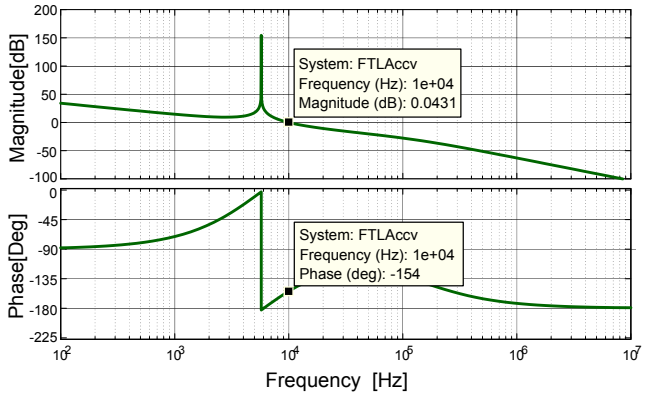


Fig. 9. Bode diagram of the closed loop system of the output voltage.

## B. Phase Shift Controller Design

The phase-shift controller is designed using the transfer function (10), which is based on the Gyrator's theory applied to Dual Active Bridge converters [22].

$$\frac{V_{DC,i}(s)}{\varphi(s)} = \left[\frac{V_{DC,i}}{\omega_c \cdot L_t} \cdot \varphi \cdot \left(1 - \frac{|\varphi|}{\pi}\right)\right] \cdot \frac{R_{o,i}}{R_{o,i}.C_{o,i} \cdot s + 1} \qquad (10)$$

For crossover frequency of 120Hz and phase margin of 60°, the PI type-II controller is designed. The zero is placed at the frequency of 32,75Hz and the polo at the frequency of 439,73Hz. Fig. 10 shows the bode diagram of the open loop transfer function with the voltage controller.

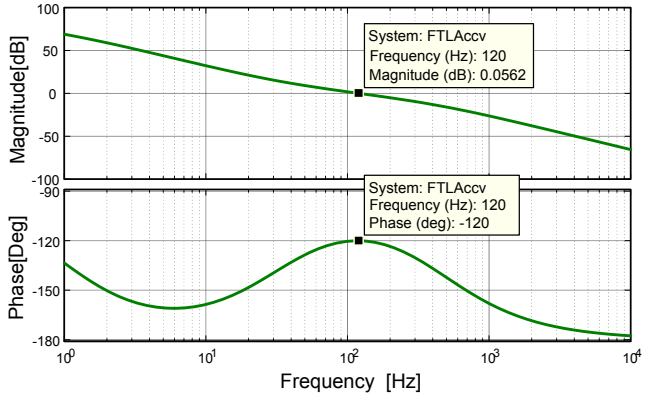


Fig. 10. Bode diagram of the closed loop system of the phase-shift control.

## C. Magnetizing Current Controller Design

The design of the magnetizing current controller is the same as in section VI.

## VIII. Simulation Results

In this section are presented simulation results obtained in the PSIM software. Fig. 11 shows the input voltage, the input current and the output voltage. The power factor is 0,994 and the Total Harmonic Distortion (THD) of the input current is 3,96%. The output voltage has the rms value of 110V and THD of 1,25%. In the same figure shows the current ripple in the input inductor as required specifications in Table II.

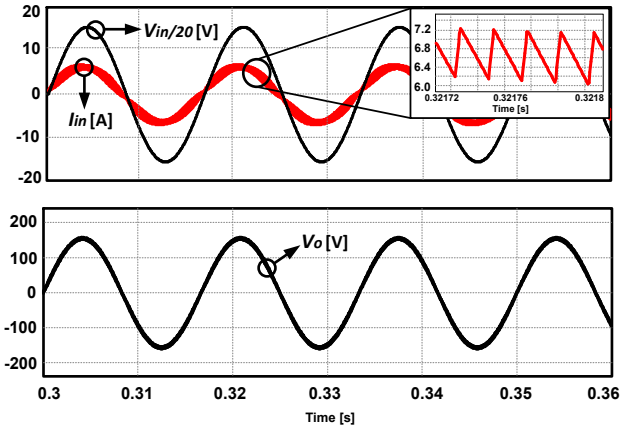


Fig. 11. Input voltage, input current, and output voltage.

The rectifier and inverter dc bus voltages are shows in Fig. 12. The balance of the voltages in the capacitors of the rectifier can also be seen. Fig. 13 shows the primary and secondary voltages and the secondary current for output power of 1kW.

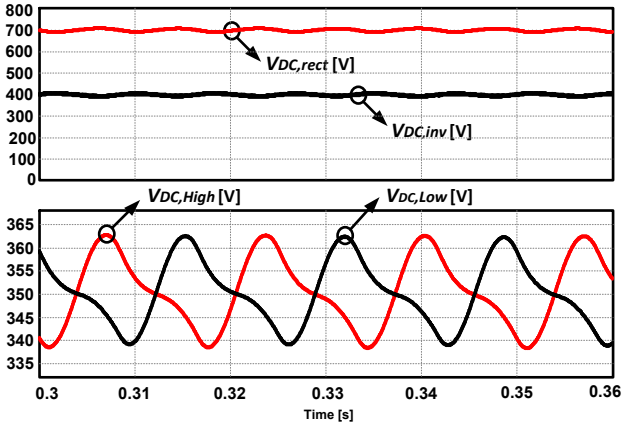


Fig. 12. DC bus voltage of the rectifier and inverter.

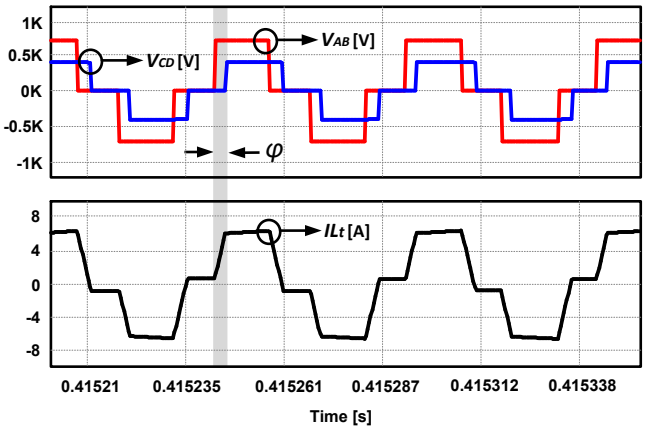


Fig. 13. Primary and secondary transformer voltages and secondary current.

The results for step-down of 50% in the output power can be seen in Fig. 14. The phase shift angle is reduced from 30° to 15°, approximately. The voltage controller ensured the inverter dc bus voltage at 400V. These results evidence the accurate operation of the inverter dc bus voltage control loop, because at the instant of the step-down of output power, the voltage follows the voltage reference after a stabilization time of 200 milliseconds.

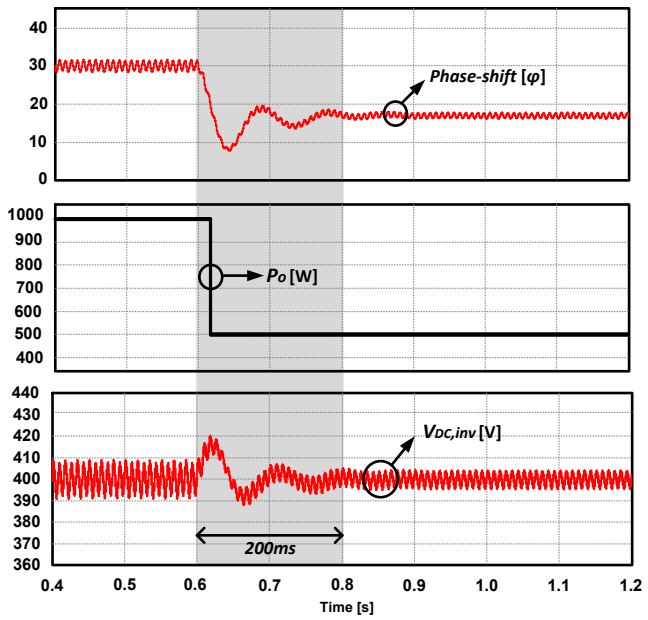


Fig. 14. Response to step-down of 50%.

Figure 15 shows the behavior of the output voltage of the AC-AC converter for a input sag voltage of 40% and time duration of 3 cycles. The output voltage is not changed with input disturbance. Thus, the proposed converter has voltage compensation feature.

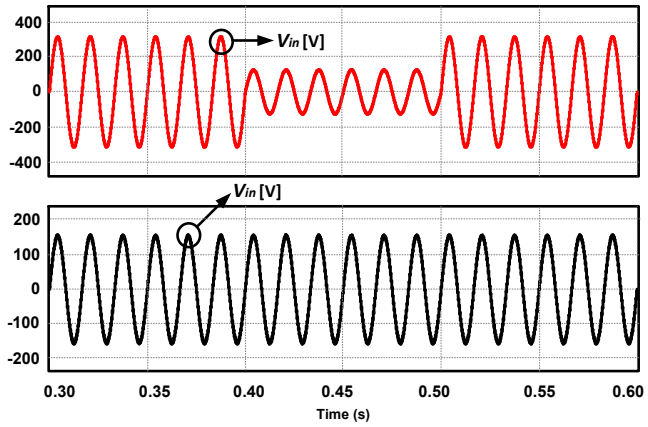


Fig. 15. Output voltage for input voltage sag.

## IX. Experimental Results

A prototype has been developed in the laboratory and some preliminary results were obtained. Table IV shows the components used in the experimental prototype. The controllers developed in section VI are discretized and implemented on Digital Signal Processor (DSP) TMS320F28377S developed by Texas Instruments. Fig. 16 is a photograph of the experimental prototype.

Figures 17, 18 and 19 shows the voltage on switch S1, the voltage at the rectifier bridge and the voltage at autotransformer of the three state switching cell. The voltage at the dc bus is 400V and the voltage at the autotransformer is +200V, 0 and -200V.

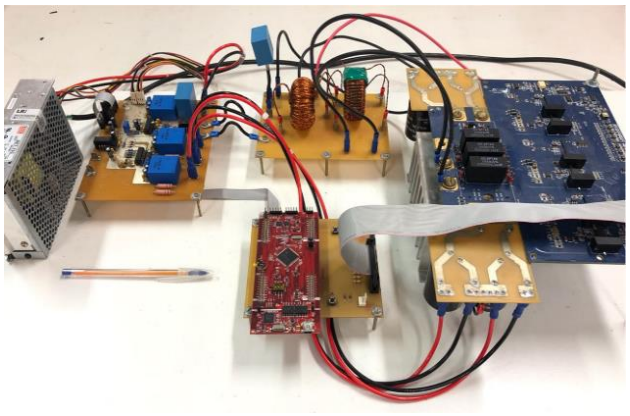

Fig. 16. Experimental prototype.

TABLE IV. Components Used in Experimental Prototype

| Components of Experimental Prototype | | | |
|---|---|---|---|
| ***Component*** | ***Model*** | ***Quant.*** | ***Specific.*** |
| Modules SiC (Cree) | CCS020M12CM2 | 2 units. | 1,2kV/20A |
| Driver (Cree) | CGD15FB45P | 2 units. | - |
| Rectifier DC Bus Capacitors | B43503-S5477-M91 | 4 units. | 470µF/450V |
| Inverter DC Bus Capacitors | B43509-G2477-M060 | 4 units. | 470µF/250V |
| LC Filter Capacitor | B32674D4225 | 1 unit. | 2,2µF/630V |
| Current Transducer | HO 25-NP/SP33<br>HO 8-NP/SP33 | 1 unit.<br>2 units | - |
| Voltage Transducer | LV 20-P | 6 units. | - |
| Iron Powder Toroidal Core (Magmattec) | MMT034T4416 | 2 units. | - |
| Ferrite Toroidal Core (Magmattec) | MMT140T5020 | 2 units. | - |
| Ferrite EE Core (Magmattec) | MMT140EE4220 | 2 units. | - |

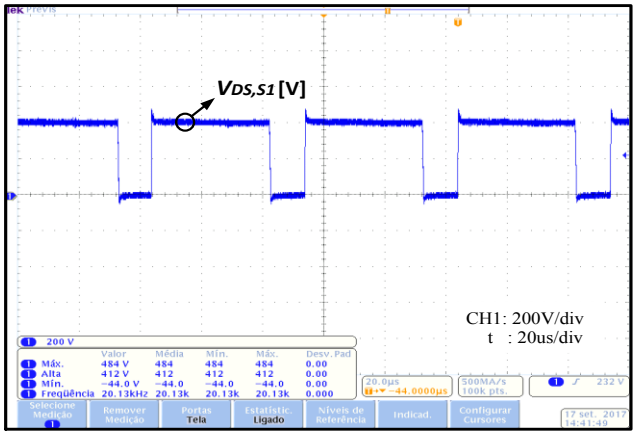


Fig. 17. Voltage on switch S1.

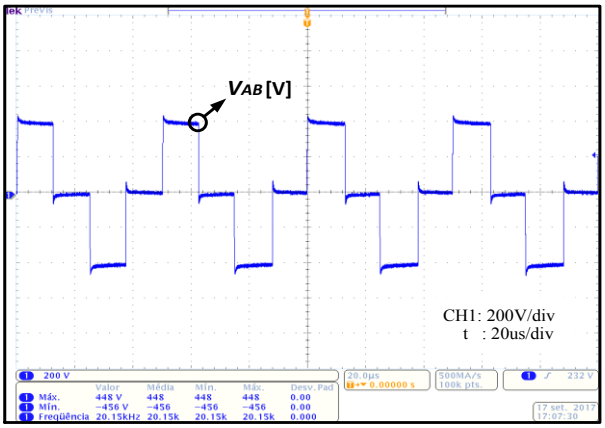


Fig. 18. Voltage at the rectifier bridge.

The input current and dc bus voltage are shown in Fig. 20. Notice that the control guarantees sinusoidal grid currents and balanced voltage across the capacitors.

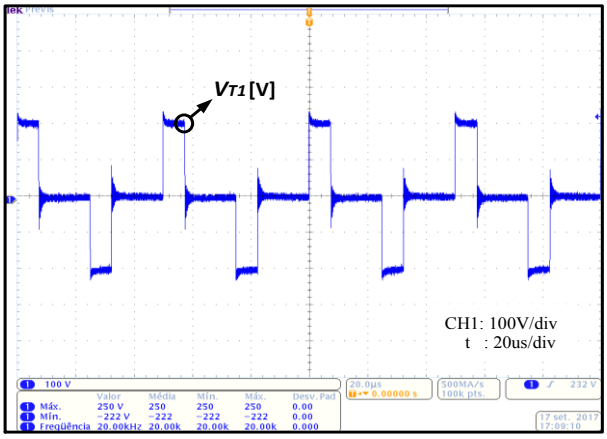


Fig. 19. Voltage at autotransformer of three-state switching cell.

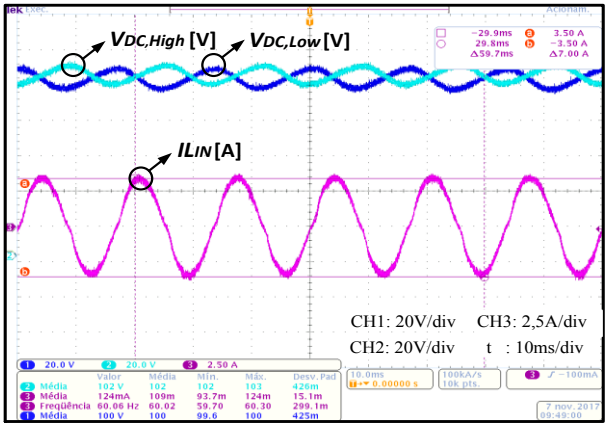


Fig. 20. Input current and voltage across the capacitors of dc bus.

## X. Conclusion

This paper presented an indirect AC-AC converter with power factor correction and high frequency insulation, based on the DAB converter and 3SSC. Initially, the modulation technique employed and the determination of the passive components of the rectifier and inverter were presented. The design of the controllers used in the simulation and experimental prototype was developed in detail. An experimental prototype has been developed and its preliminary results was presented. Full results will be presented in the final version of this paper.

## Acknoledgements

The authors acknowledgements the Energy and Control Processing Group (GPEC), Brazilian National Council for Research and Development (CAPES) and Coordination of Improvement of Higher Education Personnel (CNPq).

## References

[1] H. F. Ahmed, H. Cha, A. A. Khan, H. Kim, "A Family of High-Frequency Isolated Single-Phase Z-Source AC-AC Converters With Safe-Commutation Strategy", IEEE Transactions on Power Eletronics, vol .31, pp. 7522-7533, November 2016.

[2] H. F. Ahmed, H. Cha, A. Ali Khan, H. Kim, "A Novel Buck-Boost AC-AC Converter With Both Inverting and Noninverting Operations and Without Commutation Problem," IEEE Transactions on Power Eletronics, vol .31, pp. 5655-5665, June 2016.

[3] C. A. Petry, "Estabilizadores de Tensão para Alimentação de Cargas Não-Lineares: Estudo de Variações Topológicas e Métodos de Controle", Tese (Doutorado em Engenharia Elétrica)-INEP-UFSC,Florianópolis, 2005.

[4] Julio C. Rosas-Caro, F. Macilla-David, J. M. Gonzalez-Lopez, L. M. Ramirez-Arredondo,A. Gonzalez-Rodriguez, N. Salas-Cabrera,"A Review of AC Choppers," 20th International Conference on Electronics Communications and Computers (CONIELECOMP), 2010.

[5] D. Floricau, "PWM AC Choppers: Basic Topologies and Applications," Scientific Bulletin, Series C, vol. 68, pp. 91-106, 2006.

[6] L.A.C. Lopes, G. Joos, "Pulse Width Modulation Capacitor for Series Compensation", IEEE Transactions on Power Eletronics, vol .16, pp.167-174, March 2001.

[7] P. W. Wheeler, J. Rodríguez, Jon C. Clare, "Matrix Converters: A Technology Review", IEEE Transactions on Power Eletronics, vol .49, pp.276-289, April 2002.

[8] T. Friedli, J. W. Kolar, "Comprehensive Comparison of Three-Phase AC-AC Matrix Converter and Voltage DC-Link Back-to-Back Converter Systems", The 2010 International Power Electronics Conference – ECCE - ASIA, pp. 2789-2798, 2010.

[9] J. W. Kolar, T. Friedli, J. Rodriguez, P. W. Wheeler, "Review of Three-Phase PWM AC-AC Converter Topologies", IEEE Transactions on Power Eletronics, vol .58, pp.4988-5006, November 2011.

[10] S. Kim, S. Siul, T. A. Lipo "AC/AC Power Conversion Based on Matrix Converter Topology With Unidirectional Switches", IEEE Transactions on Industry Applications,vol. 36 pp. 139-145, January/February 2000.

[11] Congwei. Liu, Bin Wu, Navid. R. Zargari, Dewei Xu, J. Wang, "A Novel Three-Phase Three-Leg AC/AC Converter Using Nine IGBTs", IEEE Transactions on Industry Applications,vol. 24, pp. 1151-1160, May 2009.

[12] C. B. Jacobina, I. S. de Freitas, E. R. C. da Silva, A. M. N. Lima and R. L. A. Ribeiro, "Reduced Switch Count DC-Link AC-AC-Five-Leg Converter", IEEE Transactions on Power Eletronics, vol .21, pp.1301--1310, September 2006.

[13] Luan C. S. Mazza, Demercil S. O. Jr, Fernando L. M. Antues, Diego B. S. Alves, José J. S. Souza, "A Soft Switching Bidirectional DC-DC Converter With High Frequency Isolation", IEEE 13th Brazilian Power Eletronics Conference and 1st Southern Power Electronics Conference (COBEP/SPEC), 2015.

[14] R. W. De Doncker, D. M. Divan, M. H. Kheraluwala,"A three-phase soft-switched high power density DC/DC converter for high power applications", IEEE Trans. On Industry Applications, Vol 27, pp 63-73, Jan/Feb. 1991.

[15] G. V. Torrico Bascopé and I. Barbi, "Generation of a Family of Non-Isolated DC-DC PWM Converters Using New Three-State Switching Cells", in IEEE Power Eletronics Specialists Conference, 2000, pp 858-863.

[16] G. V. Torrico-Bascopé, I. Barbi, "A single phase PFC 3kW converter using a three-state switching cell", Power Eletronics Specialists Conference, 2004, PESC 04, 2004 IEEE 35th Annual,vol.5, pp4037-4042,Vol.5,20-25 June 2004.

[17] Haimin.T, Kotsopoulos.A, Duarte J. L,"Tripe-half-brigde bidirectional converter controleed by phase shift and PWM", in: Applied Power Eletronics Conference and Exposition,2006. APEC'06. Twenty-First Annual IEEE,vol., p. 7,pp 19-23, 2006.

[18] Lloyd Dixon, “Average Current Mode Control of Switching Power Supplies”, presented at the Unitrade Power Supply Design Seminar, 1990.

[19] B. R. de Almeida, J. W. M. de Araújo, P. P. Praça and D. de S. Oliveira, "A Single-Stage Three-Phase Bidirectional AC/DC Converter With High-Frequency Isolation and PFC", in IEEE Transactions on Power Electronics, vol. 33, no. 10, pp. 8298-8307, Oct. 2018.

[20] Venable. H. D, “The K-Factor: A New Mathematical Tool for Stability Analysis and Synthesi”, Proc. of Powercon 10, 1983. San Diego, USA, Conference Publications.

[21] F. Gerent, “Metodologia de Projeto de Inversores Monofásicos de Tensão Para Cargas Não-Lineares”, Dissertação de Mestrado, Universidade Federal de Santa Catarina, 2005.

[22] Barazarte. R. Y, Gonzalez. G. G, Ehsani M, “ Generalized Gyrator Theory”, IEEE Transactions on Power Eletronics, vol. 25, pp. 1832-1837, 2010.